

Short communication

# Novel polymer electrolytes based on triblock poly(ethylene oxide)-poly(propylene oxide)-poly(ethylene oxide) with ionically active SiO<sub>2</sub>

Xiao-Liang Wang, Ao Mei, Xin-Lu Li, Yuan-Hua Lin, Ce-Wen Nan\*

Department of Materials Science and Engineering, and State Key Laboratory of New Ceramics and Fine Processing, Tsinghua University, Beijing 10084, China

Received 21 March 2007; received in revised form 6 June 2007; accepted 12 June 2007

Available online 22 June 2007

## Abstract

A novel polymer electrolyte based on triblock copolymer of poly(ethylene oxide)-poly(propylene oxide)-poly(ethylene oxide) with *ionically active* SiO<sub>2</sub> inclusions has been designed. The electrolyte shows favorable features for ion migration such as low glass transition temperature and high concentration of amorphous phase. Combined with the effect of *active* SiO<sub>2</sub>, its ionic conductivity is about  $8.0 \times 10^{-5} \text{ S cm}^{-1}$  at 30 °C, which exceeds that for the PEO-based systems. As applying them to cells with LiFePO<sub>4</sub>-type cathodes, a capacity of about 147.0 mAh g<sup>-1</sup> is obtained at 60 °C, which is retained by more than 90% after 40 charge/discharge cycles. Moreover, about 100 mAh g<sup>-1</sup> could still be delivered as temperature decreases to 30 °C.

© 2007 Elsevier B.V. All rights reserved.

**Keywords:** Polymer electrolytes; Lithium batteries; Triblock copolymer; *Ionically active* SiO<sub>2</sub>; Ionic conductivity

## 1. Introduction

Electrolytes which act as ionic conductors but electronic insulators play an important role in lithium battery technology. Ionically conducting polymer membranes (polymer electrolytes) have received extensive studies due to their superior performance at elevated temperature, stability towards the lithium metal anode and safety. Applications in electric traction and backup power have already been established [1–3]. One of the most interesting systems is based on poly(ethylene oxide) (hereafter abbreviated as PEO), in which lithium ions could be coordinated with ether oxygen atoms through Lewis acid–base interactions and transported by the segmental movement of polymer. The practically useful ionic conductivity (of about  $10^{-4} \text{ S cm}^{-1}$ ) could be achieved at temperatures of 60–80 °C. However, the tendency to crystallize and poor polymer chain dynamics lead to inferior performance at lower temperature (e.g., the ambient conductivity is around  $10^{-7} \text{ S cm}^{-1}$  for the archetypal PEO–LiClO<sub>4</sub> systems) [4–7].

Recently, great attention has been paid to extend the operation temperature range of the polymer electrolytes in the hope of powering portable devices as well as application in cold weather. Several approaches have been explored to suppress the crystallization of polymer and promote chain movement in order to enhance the ionic conductivity. An effective strategy involves molecular design through copolymerization of two or more monomer species [8–10]. The different constitutive monomers influence the symmetry of polymer chains, resulting in a high degree of localized amorphous regions. In this case, at least one of the monomers should have an ability to dissolve lithium salts. Alternatively, the crystallization of polymer electrolytes can be inhibited by adding inorganic powders [4,11–15]. It is suggested that the fillers may serve as the cross-linking centers for polymer segments as a result of the interaction between the Lewis acid agents attaching to the surfaces of particles and the Lewis base atoms on polymer chains, thus preventing the polymer from reorganization.

In the present work, by combining the beneficial effects of copolymerization and composite on the ionic conductivity enhancement, polymer electrolytes based on a triblock copolymer of (EO)<sub>m</sub>–(PO)<sub>n</sub>–(EO)<sub>m</sub> (where PO is the abbreviation of propylene oxide) with *ionically active* SiO<sub>2</sub> have been designed.

\* Corresponding author. Tel.: +86 10 6277 3587; fax: +86 10 6277 3587.  
E-mail address: [cwnan@tsinghua.edu.cn](mailto:cwnan@tsinghua.edu.cn) (C.-W. Nan).

$(EO)_m-(PO)_n-(EO)_m$  with different values of  $m$  and  $n$  forms a class of copolymers which has been recently explored as amphiphilic templates for various ordered mesoporous silica synthesis, utilizing the effect of self-assembly of the hydrophilic EO blocks and the hydrophobic PO blocks under certain conditions [16]. Of interest to note, these copolymers also possess structures similar to PEO, i.e., ether oxygen atoms existing in the chains, which implies possibility to be employed in the polymer electrolytes. Here, one kind of these triblock copolymers with a formula of  $(EO)_{20}-(PO)_{70}-(EO)_{20}$  (P123) was used as the matrix. *Ionicity active*  $\text{SiO}_2$  which was designed by confining liquid electrolytes in nano-sized channels of SBA-15 (a kind of mesoporous  $\text{SiO}_2$  also prepared using P123 as the template) was dispersed in this matrix. High ionic conductivity is achieved and can be a potential candidate for use in the lithium batteries.

## 2. Experimental

Mesoporous SBA-15 powder was synthesized by hydrolysis and condensation of tetraethoxysilane (TEOS) as the silicon source in presence of P123 as the template, according to the method reported by Zhao et al. [16]. The resultant particles (Fig. 1) have two-dimensional ordered pores with an average diameter of about 10 nm and specific Brunauer–Emmett–Teller surface area of about  $956 \text{ m}^2 \text{ g}^{-1}$ . For preparing *ionically active*  $\text{SiO}_2$ , the mesoporous particles were immersed into  $1 \text{ M Li}[(\text{CF}_3\text{SO}_2)_2\text{N}]$  (LiTFSI)/[ethylene carbonate (EC) + propylene carbonate (PC) (1:1 by weight)], and the suspension was stirred for 4 days with ultrasonation so as to fill in the nanopores. Then the powder was filtrated and dried to remove the residual liquid. For polymer electrolytes preparation, the calculated amount of P123, LiTFSI and *active*  $\text{SiO}_2$  were dissolved and dispersed in acetonitrile. Then the samples were dried and further annealed in vacuo at  $80^\circ\text{C}$  for 5 h. For comparison, the pure P123–LiTFSI samples and P123– $\text{LiClO}_4$  samples were also prepared in the same way. The samples were denoted as  $(\text{P123})_n\text{-LiX}/m\%$ , where  $n$  represents the molar ratio of ether O in P123 to lithium atoms in lithium salts (i.e.,  $n(\text{O})/n(\text{Li})$ ) and  $m\%$  represents the amount of *active*  $\text{SiO}_2$  added to the total  $(\text{P123})_n\text{-LiX}$  weight. Moreover, the  $\text{LiFePO}_4$  type cathode films

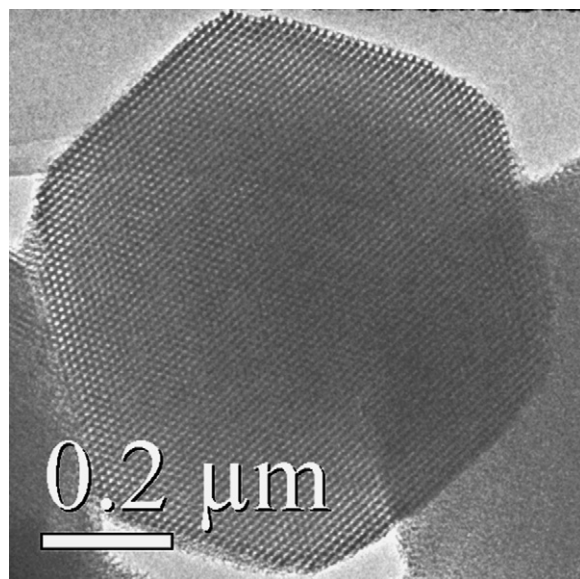


Fig. 1. TEM morphology of SBA-15 particles.

were prepared by blending the  $\text{LiFePO}_4$  active material (90 wt%) with carbon black (5 wt%) and a PVDF binder (5 wt%), using Al foils as current collector. The  $\text{LiFePO}_4$  surface loading is about  $4.1 \text{ mg/cm}^2$ . The 2032-type coin cells in which the polymer electrolytes sandwiched between  $\text{LiFePO}_4$  cathodes and lithium metal anodes with the help of polyolefin separators (Celgard) were assembled in glove box.

The morphology of SBA-15 particles was investigated by JEM-2011 transmission electron microscopy (TEM). Differential scanning calorimetry (DSC) was measured using DuPont TA 2910-modulated DSC at a heating rate of  $10^\circ\text{C}/\text{min}$ . The complex Electrochemical Impedance Spectroscopy (EIS) of the samples sandwiched between stainless steel (SS) blocking electrodes were measured in Ar atmosphere using Chenhua CHI760B Electrochemical Workstation. The battery performance was tested by Land 2001A battery test system at different temperatures. The voltage for charge-discharge cycling is set between 2.50 V and 3.95 V. The value of current density is described as  $C/t$ , which means total charge or discharge of the cells in  $t$  hours. Larger  $t$  represents smaller current density.

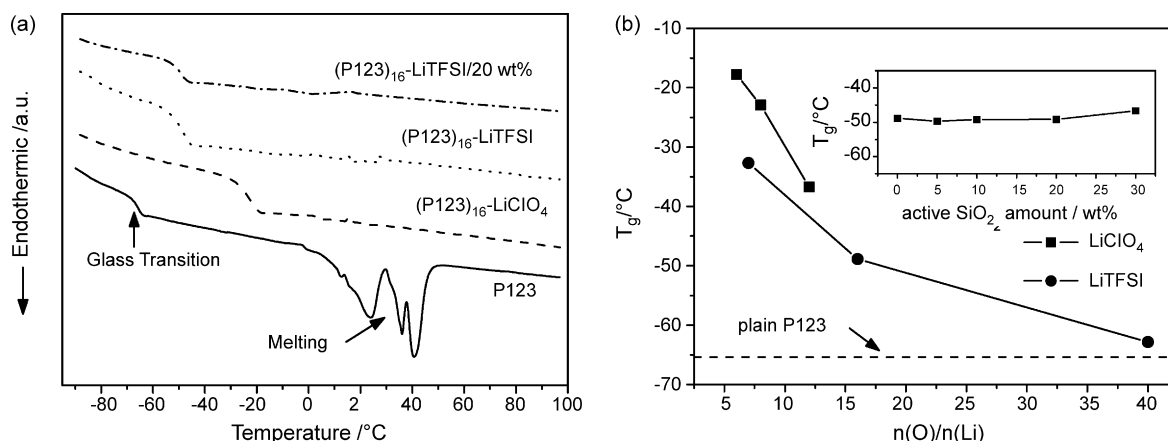


Fig. 2. (a) DSC traces, and (b) the  $T_g$  values of the samples containing different lithium salts and *ionically active*  $\text{SiO}_2$ .

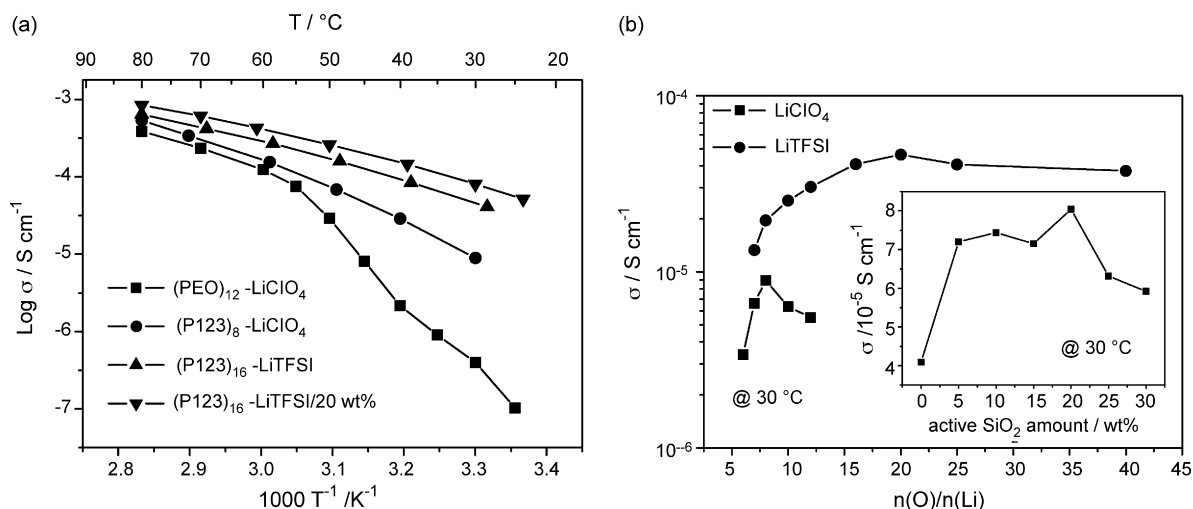


Fig. 3. Variation of ionic conductivity of the polymer electrolytes with (a) temperature, and (b) the salt concentration and *ionically active* SiO<sub>2</sub> amount at 30 °C.

### 3. Results and discussion

The chain organization and segmental mobility of polymer electrolytes could be reflected in DSC studies. As shown in Fig. 2a, for the plain P123, there are several endothermic peaks between 10 °C and 50 °C due to the melting of polymer, which implies co-existence of different crystalline phases. Moreover, the step around -65.4 °C indicates the transition of the sample from a glass state to a rubbery state at higher temperature (i.e., the glass transition temperature  $T_g$ ). After doping LiClO<sub>4</sub>, the endothermic peaks disappear, suggesting the nearly total amorphous feature at room temperature, which may be caused by the cross-linking effect of lithium ions interact with oxygen atoms in the chains (one lithium ion can coordinate with four oxygen atoms) [11]. However, this effect also leads to the stiffening of chains, thereby increasing  $T_g$  to -22.9 °C. By substituting LiClO<sub>4</sub> with LiTFSI, the  $T_g$  value of polymer electrolytes is obviously lowered, and the disordered structure is retained simultaneously. The plasticization of polymer electrolytes could be induced by the macro anion TFSI, which holds large delocalized electric charge and has less ability to bond lithium ions.

It should be mentioned that the  $T_g$  value increases as the salt concentration increases in both systems as shown in Fig. 2b. Furthermore, the dispersion of *active* SiO<sub>2</sub> in P123–LiTFSI systems does not deteriorate the chain dynamics (see the inset in Fig. 2b).

Fig. 3 shows the ionic conductivities of P123 based systems and PEO based systems. As seen from Fig. 3a, the ionic conductivity of PEO based system usually increases with temperature and has a break around its melting point  $T_m$  (~53 °C). The existence of crystalline regions and the low segmental dynamics below  $T_m$  lead to its low ionic conductivity around room temperature. The comparison in Fig. 3a illustrates that P123-based electrolytes exhibit different behavior, i.e., no break occurring over the whole measuring temperature range, which is attributed to the suppression of crystallization. The pronounced conductivity enhancement around room temperature clearly confirms the beneficial role of P123. In the P123–LiTFSI samples, the promoted segmental kinetics and the high dissolution tendency of the salt lead to higher ionic conductivity compared with the ones containing LiClO<sub>4</sub>. Moreover, a further enhancement is achieved by the introduction of *active* SiO<sub>2</sub>. Concerning the

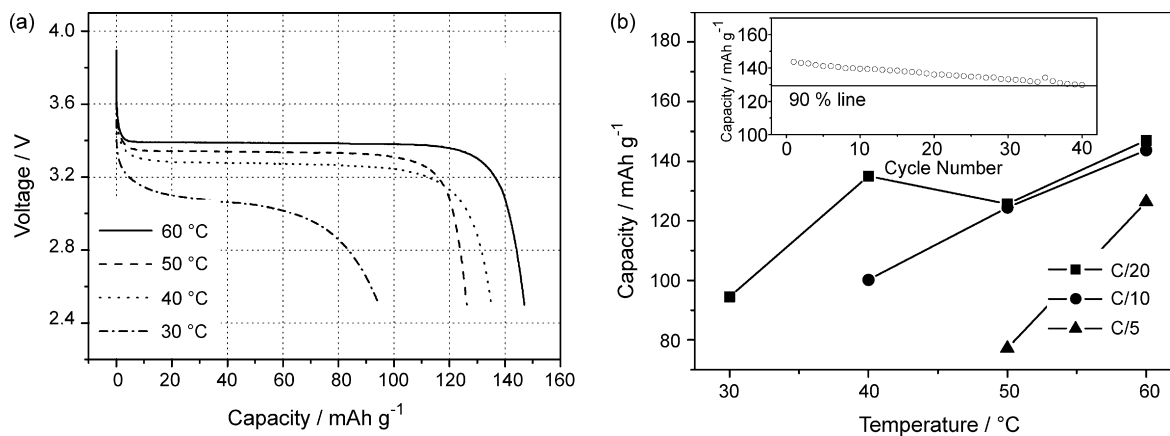


Fig. 4. (a) Discharge profiles of the cells of LiFePO<sub>4</sub>/[(P123)<sub>16</sub>-LiTFSI/20 wt%]/lithium metal, at various temperatures and at a current density of 0.026 mA/cm<sup>2</sup> (~C/20). (b) Discharge capacities at various temperatures and at different current densities, where the inset shows the capacity profile during cycling at 60 °C and at 0.051 mA/cm<sup>2</sup> (~C/10).

amorphous state of the pure P123–LiTFSI systems, this increase is mainly due to the fast transport path through the nanochannels filled by liquid electrolytes [12]. The salt concentration also has an impact on ionic conduction as shown in Fig. 3b. The increase of LiClO<sub>4</sub> content can promote the charge carrier concentration, but elevate  $T_g$  as well (see Fig. 2b). Besides, our Infrared Spectra studies identified a sharp decline of free ions ratio as  $n(\text{O})/n(\text{Li})$  approaches 6 (not presented here). These competing effects cause the high ionic conductivity to be achieved at the moderate concentration of  $n(\text{O})/(\text{Li})=8$ . It is worth to note that the high ionic conductivity of the systems with LiTFSI can be obtained with relatively lower salt addition and preserved as the salt concentration further decreases. As active SiO<sub>2</sub> is added, the ionic conductivity reaches to about  $8.0 \times 10^{-5} \text{ S cm}^{-1}$  at 30 °C and  $4.3 \times 10^{-4} \text{ S cm}^{-1}$  at 61 °C for (P123)<sub>16</sub>–LiTFSI/20 wt% samples, respectively (see the inset in Fig. 3b). The value at 30 °C is about three times higher than that achieved by sol-gel self-assembled (EO)<sub>106</sub>–(PO)<sub>70</sub>–(EO)<sub>106</sub> and mesoporous SiO<sub>2</sub> systems [9]. Further increase of the active SiO<sub>2</sub> results in blocks of aggregation, thus hindering the ionic conduction.

In order to investigate the capability of the P123-based electrolytes serving as polymer electrolytes, cycling testing was performed. LiFePO<sub>4</sub> type cathode which displays a discharge voltage plateau of ~3.4 V (vs. Li) is employed to assure the cycling between 2.5 V and 3.95 V. Typically, a discharge capacity of about 140 mAh/g could be obtained in the practical cycling which is slightly lower than the theoretical capacity (i.e., 170 mAh/g) [17]. As shown in Fig. 4, the cells with a configuration of LiFePO<sub>4</sub>//[(P123)<sub>16</sub>–LiTFSI/20 wt%]/lithium metal can cycle successfully in the temperature range studied. A flat and high voltage discharge plateau has been achieved at 60 °C with a capacity of more than 140 mAh/g (see Fig. 4a). As the current density increases to 0.102 mA/cm<sup>2</sup> (~C/5), over 120 mAh/g is still sustained (Fig. 4b). These capacity features are much better than the PEO-based polymer electrolytes. For example, the PEO-based composite polymer electrolytes containing superacid ZrO<sub>2</sub> only achieved a capacity of about 60 mAh/g with LiFePO<sub>4</sub> type cathode using a current density of C/7 at 60 °C [18]. Nevertheless, the cells with P123-based polymer electrolytes also show good capacity retention during cycling. As shown in the inset of Fig. 4b, after 40 cycles at a discharge current density of 0.051 mA/cm<sup>2</sup> (~C/10) at 60 °C, the capacity decay is lower than 10% of the initial value. In addition, cycling can be performed with the coulomb efficiency approaching 100%. Although the capacity tends to decline as temperature decreases, which may be due to the increasing internal resistance as reflected by the enlarged polarization, the cells can still deliver a capacity of about 94.4 mAh/g at 30 °C.

#### 4. Conclusions

A novel kind of composite polymer electrolytes containing (EO)<sub>20</sub>–(PO)<sub>70</sub>–(EO)<sub>20</sub> triblock copolymer, ionically active SiO<sub>2</sub> inclusions and LiTFSI has been designed. The electrolytes show favorable features. Ionically active SiO<sub>2</sub> particles also facilitate ion transport through the ordered nanochannels filled by liquid electrolytes. Their ionic conductivity is much higher than that of PEO-based systems. As the (P123)<sub>16</sub>–LiTFSI/20 wt% polymer electrolytes are applied to cells with LiFePO<sub>4</sub>-type cathodes and lithium metal anodes, a capacity of 147.0 mAh/g is obtained at 60 °C, and the cells display good capacity retention with high coulomb efficiency during cycling. Moreover, 94.4 mAh/g is still retained as temperature decreases to 30 °C. Further enhancement in ionic conductivity and cell properties would be expected by optimizing the ratio of EO and PO moieties in the copolymer matrix.

#### Acknowledgement

This work was supported by the NSF of China. The authors would like to thank Prof. Q. Cai and Dr L. Zou for helpful discussions.

#### References

- [1] J.M. Tarascon, M. Armand, Nature 414 (2001) 359.
- [2] A.S. Arico, P. Bruce, B. Scrosati, J.M. Tarascon, W. Van Schalkwijk, Nat. Mater. 4 (2005) 366.
- [3] A. Ritchie, W. Howard, J. Power Sources 162 (2006) 809.
- [4] F. Croce, G.B. Appetecchi, L. Persi, B. Scrosati, Nature 394 (1998) 456.
- [5] B. Scrosati, C.A. Vincent, MRS Bull. 25 (2000) 28.
- [6] P.V. Wright, MRS Bull. 27 (2002) 597.
- [7] A.J. Bhattacharyya, J. Fleig, Y.G. Guo, J. Maier, Adv. Mater. 17 (2005) 2630.
- [8] M. Watanabe, A. Nishimoto, Solid State Ion. 79 (1995) 306.
- [9] H.M. Kao, C.L. Chen, Angew. Chem. Int. Ed. 43 (2004) 980.
- [10] T. Niitani, M. Shimada, K. Kawamura, K. Kanamura, J. Power Sources 146 (2005) 386.
- [11] W. Wieczorek, K. Such, Z. Florjanczyk, J.R. Stevens, J. Phys. Chem. 98 (1994) 6840.
- [12] C.W. Nan, L.Z. Fan, Y.H. Lin, Q. Cai, Phys. Rev. Lett. 91 (2003) 266104.
- [13] Y. Tominaga, S. Asai, M. Sumita, S. Panero, B. Scrosati, J. Power Sources 146 (2005) 402.
- [14] J.H. Shin, F. Alessandrini, S. Passerini, J. Electrochem. Soc. 152 (2005) A283.
- [15] X.L. Wang, A. Mei, M. Li, Y.H. Lin, C.W. Nan, Solid State Ion. 177 (2006) 1287.
- [16] D.Y. Zhao, J.L. Feng, Q.S. Huo, N. Melosh, G.H. Fredrickson, B.F. Chmelka, G.D. Stucky, Science 279 (1998) 548.
- [17] A.K. Padhi, K.S. Nanjundaswamy, J.B. Goodenough, J. Electrochem. Soc. 144 (1997) 1188.
- [18] F. Croce, S. Sacchetti, B. Scrosati, J. Power Sources 162 (2006) 685.